Conf-950226--4

SAND94-2145C

HIGH ENERGY ELECTRON BEAMS FOR CERAMIC JOINING

B. N. Turman, S. J. Glass, J. A. Halbleib, D. R. Helmich, R. E. Loehman, Sandia National Laboratories, Albuquerque, NM, 87185; J. R. Clifford, Titan Corporation, Albuquerque, NM, 87106

ABSTRACT

Joining of structural ceramics is possible using high melting point metals such as Mo and Pt that are heated with a high energy electron beam, with the potential for high temperature joining. A 10 MeV electron beam can penetrate through 1 cm of ceramic, offering the possibility of buried interface joining. Because of transient heating and the lower heat capacity of the metal relative to the ceramic, a pulsed high power beam has the potential for melting the metal without decomposing or melting the ceramic. We have demonstrated the feasibility of the process with a series of 10 MeV, 1 kW electron beam experiments. Shear strengths up to 28 MPa have been measured. This strength is comparable to that reported in the literature for bonding silicon nitride to molybdenum with copper-silver-titanium braze, but weaker than that reported for Si_3N_4-Si_3N_4 with gold-nickel braze. The bonding mechanism appears to be a thin silicide layer.

INTRODUCTION

Ceramics such as Si_3N_4 and SiC are seeing increasing use for high temperature structural applications such as turbochargers for automobile engines, turbowheels for aircraft auxiliary power units, stator shrouds for gas turbines for power generation applications, ceramic armor, ceramic thermal protecting tiles, and high energy flux mirrors. Although ceramics are being fabricated that can survive these challenging environments, their application is still limited by the lack of suitable technologies for joining them to components such as metal shafts or for joining them to themselves. Approaches such as shrink fit, push fit, high temperature active metal brazes, and friction welding have been tried. Success has been demonstrated for braze metal joints subjected to low or moderate temperatures. For example a Si_3N_4 turbocharger rotor was joined to Incoloy 903 with an active metal braze with triple-laminated interlayers. This joint was designed to see a maximum operating temperature of 550°C (1030°F) [1]. A limitation of most joining techniques is that they require that the parts be exposed to high temperatures, which may result in degradation in the performance of the metal component. Although localized heating is possible using lasers this technique is not applicable to buried interfaces. Thus alternative joining techniques are being explored.

Low energy electron beams produced by electron beam welders with energies in the range of 20-150 keV, have been used to join ceramics in a limited number of experiments. Hokanson et al. used an electron-beam welder with 55-130 keV, 0.05-3.0 ma, a welding speed of 5-30 in/min., and a power of 3 kW [2]. Bending strengths of 19.7 ksi (136 MPa) were achieved for alumina-alumina joints. They were also able to achieve joints of

96% alumina to W, Mo, Nb, and Kovar. Rice reported results for electron-beam welded alumina [3]. There were problems with cracking and repeatability but strengths of 42-197 MPa for alumina to alumina joints, and 42 MPa for Ta to alumina joints were measured. Electron-beam welding of carbides did not show much promise because of decomposition or vaporization. Charge build-up did not appear to be a problem because of the combination of high temperature conductivity, electron emission, and nearby supplemental heaters that prevented such a buildup. The success of these electron-beam joining efforts appears to have been limited by the shallow penetration of the electron beam (0.1 mm). This necessitates heat transfer to the adjoining material by conduction which is notoriously poor in most ceramics. Thermal stresses due to large thermal gradients often lead to fracture of the ceramics.

Using electron beams with accelerating potentials of 2-10 MeV could alleviate some of these problems. Energy deposition is much deeper and more uniform through the bulk of the ceramic, potentially leading to the elimination of both of the problems encountered using lower energy electron beam joining efforts. The objective of our present work was to evaluate the feasibility of high energy electron beam joining of ceramics using refractory metals such as Pt and Mo, using the deep penetration and transient thermal characteristics that can be achieved with a high energy, high power electron beam.

OPERATING REGIMES FOR MATERIALS PROCESSING WITH HIGH ENERGY BEAMS

The effect of electron or laser beams on materials depends on both the properties of the material and the beam parameters. The materials properties of primary interest are the absorptivity and thermal diffusivity. The beam parameters of interest are the beam power, diameter, energy or wavelength, pulse frequency, and interaction time. As a point of reference, Jasim et al, studied operating regimes for laser surface engineering of zirconia ceramics [4]. Jasim also reported on previous work on metal processing using lasers. The following power regimes were identified:

1.	Metal heating without melting at	$\sim < 10^4$ W/cm^2.
2.	Metal melting at	$\sim 10^4 - 10^6$ W/cm^2.
3.	Ceramic sealing	$\sim 10^3 - 10^4$ W/cm^2.
3.	Metal evaporation at	$\sim 10^6 - 10^8$ W/cm^2.
4.	Plasma formation at	$\sim > 10^8$ W/cm^2.

Laser sealing was the melting of the top layer of a plasma sprayed zirconia coating. Sealing required a laser power density of 5100 W/cm^2 for 12.5 ms. The difference between metals and ceramics is largely due to the lower absorptivities and higher diffusivities of the metals. From these data, we would expect that a power density in the range of $10^3 - 10^4$ W/cm^2 would be required for ceramic joining, a conclusion that is verified by our experiments.

ELECTRON ENERGY ABSORPTION IN MATERIALS

Figure 1 illustrates the geometry of our experiment, in which an electron beam is incident on the sample from the top. Differential electron beam absorption in matter is governed by the equation:

$$dE/dx = -S(\text{MeV-cm}^2/\text{gm})\rho(\text{gm/cm}^3),$$

where S(V) is the stopping power of the electrons at energy V, and ρ is the mass density of the material. The "electron range" is the maximum penetration distance of electrons of energy V into the material. This is given approximately by

$$R=V_0/S\rho.$$

For the ranges of interest for MeV-class beams, the stopping power is about 2 MeV-cm^2/gm. A 10 MeV beam, then, has a range of about 1.5 cm in Si_3N_4 (ρ=3.44 gm/cm^3), and about 0.5 cm in molybdenum (ρ=10.22 gm/cm^3).

The temperature rise for each region, assuming no heat conduction is:

$$\Delta T = \frac{\epsilon}{C_p \ \rho a d}$$

where C_p = heat capacity,
a = unit area
d = thickness.
ϵ = deposited energy density

As the beam impulse energy is conducted into the adjacent material, the temperature differential equilibrates, on the time scale [5]

$$\tau = \frac{4d^2}{\pi^2 \alpha}$$

$$\alpha = \frac{K}{\rho c_p}$$

$$K = \textit{conductivity} = 40 \quad w/m - {}^\circ K \ (Si_3 N_4)$$

$$c_p = 0.8 \quad J/gm - K$$

$$\alpha = 0.15 \quad cm^2/s$$

$$d = 3\ mm \quad \tau = 0.24\ s$$

Energy put into the system on a time scale shorter than τ will not equilibrate temperatures between the regions. On a substantially larger time scale, temperatures are equilibrated.

When the ceramic-metal combination is heated rapidly, a temperature gradient from the inside to the outer surface occurs. This gradient can produce cracking if the stress from thermal expansion exceeds the strength of the material. The surface stress, σ, developed when a plate experiences an infinitely fast quench over a temperature ΔT is given by [6]

$$\sigma = \frac{E\alpha_x \Delta T}{1-\upsilon}$$

	Si_3N_4	$Si\,C$
E = Young's modulus	2.8×10^7 N/cm^2	4.1×10^7 N/cm^2
α_x = expansion coefficient	2×10^{-6} / °K	4×10^{-6} / °K
υ = Poisson's Ratio	0.27	0.27
σ = FractureStress	5.7×10^4 N/cm^2	6.5×10^4 N/cm^2

The maximum allowable temperature differential between the bulk and surface of the ceramic is given by

$$\Delta T = \frac{(1-\nu)}{E\,\alpha_x}\ \sigma$$

For Si_3N_4: $\Delta T_{max} =$ 738° K

The maximum absorbed energy density that can be tolerated is $\frac{\Delta\varepsilon}{a} = c_\rho\ \rho d \Delta T$

$$(\Delta\ \varepsilon/a)_{max} = (0.8)\,(3.44)(0.3)\,(738)$$

for d = 0.3 cm $(\Delta\ \varepsilon/a)_{max}$ = 610 J/cm^2 *for* Si_3N_4

This must be done on time scale of about τ, so maximum absorbed power density is

$$P_{max} = 2500 w/cm^2$$

In the actual experiment, we find that this estimate is too high by a factor of 2: the stress limit for Si_3N_4 is about 1200 w/cm^2 absorbed power.

HIGH ENERGY BEAM JOINING EXPERIMENTS

Joining experiments were conducted at 10-15 MeV, a convenient voltage because of the penetration power of almost 2 cm in ceramic, and the availability of an electron beam research facility and RF linear accelerator at Titan Corporation. This accelerator has a maximum capability of 2 kW beam power and maximum voltage of 15 MeV. A standard set up of 10 MeV, 0.18 A beam current, 6 μsec pulse width, and 11 J per pulse was used for most of the testing. Average beam power was changed in the experiment by varying the repetition frequency up to the maximum of 100 Hertz.

Experiments were conducted both in air and in vacuum. For the atmospheric air experiments, a thin titanium foil window (5 mils) was used to separate the accelerator column from atmosphere. At 10 MeV, there was no more than 4% beam energy loss in the exit foil. For the vacuum experiments, An exit foil was used to isolate the processing vacuum chamber from the accelerator column. Vaporization of sample materials during heating can produce a significant increase in vacuum pressure. Therefore, the titanium foil served to protect the accelerator from excessive outgassing.

Beam intensity profiles for the 10 MeV beam were measured using radiation darkening of glass plates. While this technique is often used for qualitative beam observations, it has not been used previously for quantitative measurements. Therefore, we first exposed a number of 3 mm-thick plates to multiple beam pulses, to produce a calibration plot of optical density versus intensity. This calibration plot is shown in Figure 2. Optical density, defined as the log of the optical transmission, was measured with a densitometer. Intensity was determined from the total beam area and the integral of the beam profile. The intensity scale is in units of 1 kJ/mm^2 beam energy density. Note that the glass darkening effect begins to saturate at a density beyond 0.2. Figure 3 is a beam profile for the 10 MeV, 0.19 A beam that was used for the ceramic joining experiments. This beam profile was obtained from an averaging of density measurements across two orthogonal scans, with the saturation correction from Figure 2. The peak beam intensity is I_{peak} = 3622 W/cm^2. The half-width of the beam, the radius which includes half of the beam power, is 2 mm. The average beam power within the half-width is $I_{1/2}$ = 3175 W/cm^2.

Si_3N_4 was obtained from Allied Signal Ceramic Components. The material was GN10 Si_3N_4 and its additives are Y_2O_3 and SrO_2. Sample dimensions were 0.5"x0.5"x0.10" and 0.5"x0.5"x0.25". The refractory metal foils were 1 or 2 mil (25 and 50 μm) thick and were cut in squares with an area of 0.5"x0.5" for sandwiching between pieces of Si_3N_4. Specimens were cleaned and then placed on top of each other with the refractory metal foil sandwiched in between. The top and bottom pieces of Si_3N_4 were offset from each other slightly to facilitate shear testing after joining. The samples were placed on top of a porous zirconia refractory plate which was then placed in a stainless steel fixture. This fixture provided an electrical path to prevent charge build-up and also allowed a light pressure to be exerted on the pieces to be joined.

EXPERIMENTAL RESULTS

Joint Shear Strength of 10 MeV Electron Beam Joined Specimens

Compressive shear strengths measured on a mechanical testing frame at a loading rate of 0.1 cm/min. The shear strength was calculated from the actual bonded area, as measured with ultrasonic inspection. The shear strength for two Pt joints were 10.5 and 11.5 MPa. The average strength for five Mo joints was 23 MPa, with a range from 11 to 28 MPa. Ultrasonic scans of the joints indicated considerable non-uniformity of the bonding, with a central region being unbonded, the adjacent region being relatively well bonded, and the outermost region being poorly bonded or unbonded.

The Mo foil from one of these samples after shear testing, is shown in Fig. 4. At the center of the beam, metal melting has occurred, but because the Mo poorly wets the Si_3N_4 (wetting angle >90°), the molten metal appears to have retreated to the edges of the unmelted metal. Surface damage to the Si_3N_4 is apparent in the region of highest power density, at the center of the beam. The bonded region occurs in an annulus of radius 1 - 2 mm, where the power density is between 1000 - 2000 w/cm^2. This appears to be the best range for beam joining, where the temperatures are sufficient to achieve bonding reactions, but low enough so that material damage is avoided.

Scanning Electron Microprobe (SEM) observations of the bonded regions of our samples suggest that the bonding mechanism is reaction bonding, rather than a simple melting, wetting, and resolidification of the metal. SEM examination of the Pt layer reveals thin reaction layers of Pt_3Si, a known Pt silicide [7],and Pt_4Si. These reaction layers, which are approximately 1-2 μm in thickness, appear to be responsible for bonding. Reaction layers of Mo_5Si_3 and $Mo_{10}Si_3$ are also observed at the interfaces between the Mo and the Si_3N_4. These are the same phases observed in hot-pressed Si_3N_4-Mo-Si_3N_4 joints [8,9].

In previous shear strength measurements, Akselsen [10] showed shear strength vs. braze temperature and shear strength vs. braze time for Si_3N_4-Si_3N_4 joints brazed with Cu-Ti alloys. He observed a maximum value of 320 MPa (46.4 ksi), but values ranged between 30 MPa and 320 MPa. Kang [11] reported shear strengths of 292 MPa for Ti-coated Si_3N_4 brazed with Au-Ni, and 311 MPa for Zr-coated Si_3N_4 brazed with Au-Ni. Mizuhara measured shear strengths of 28-36 MPa for Si_3N_4 joined to Mo with Cusil ABA braze alloy [12]. Thermal expansion mismatch stresses between the Si_3N_4 and the Mo likely contribute to the low strength of these joints. Kang reported torsional shear strengths of Si_3N_4/Ni/Incoloy 909 brazed joints of 151 MPa at room temperature and 11 MPa at 650°C. He measured the strength of Si_3N_4/Mo/Incoloy 718 joints and obtained values of 82.4 MPa at room temperature and 0.84 MPa at 950°C [13]. Thus we have achieved strengths in the low end of the range of strengths achieved for joints fabricated using conventional techniques (30-320 MPa). However, these results are for our initial experiments and are expected to improve significantly with a more uniform beam profile.

Si_3N_4 Bend Strength After Exposure to 10 MeV Electron Beam

Si_3N_4 exposed to the 10 MeV electron beam exhibits various degrees of surface damage depending on the beam power density and exposure time. Some of this damage has been in the form of craters on exposed surfaces, and uplift and cracking on joint surfaces. A surface layer of a metallic looking substance, which appears to be Si metal, has also been observed for lower beam power densities. Surface or bulk damage is expected to lead to a degradation in the strength of the Si_3N_4, and a corresponding degradation in its performance in structural applications.

Four point bend strength measurements were made on bend bars of as-received GN10 Si_3N_4, and on bend bars exposed to the 10 MeV electron beam at peak power density of 3770 W/cm^2. The mean strength of the samples exposed to the beam was 607 MPa, compared to the as-received strength of 970 MPa. Although the strength of beam-damaged Si_3N_4 represents a retained strength of only 62%, the strength after exposure is still high relative to other ceramic materials. We also expect that with further optimization of the beam parameters we should be able to reduce beam damage and achieve higher retained strengths.

MODELING SIMULATIONS

Radiation transport and heat transfer simulations were employed in support of the design and analysis of the buried layer experiments. Because the distributions of the electron sources in space, energy, and angle were assumed to be constant in time, the radiation transport could be simulated in time-independent fashion. The resulting energy disposition profiles, along with the time dependence of the source were then used as input to the heat transfer simulations which yielded the time dependent temperature profiles.

The ACCEPT code of Version 3.0 of the Integrated TIGER Series (ITS) code system [14] was used to obtain the three-dimensional energy deposition profiles in the experimental geometries. The thermal analysis code P/THERMAL was used to resolve transient temperature distributions within the computational domain [15]. Energy was allowed to radiate from the exposed faces of the ceramic to surrounding surfaces which were assumed to remain at a constant temperature of 298 ^oK. Thermo-physical properties for the various materials were modeled as temperature dependent quantities and were acquired from published data and the manufacturer's specifications. The interface between the metal and ceramic was modeled by contact resistance and gap radiation. Since the brazing experiments were carried out in an evacuated chamber and the physical clamping pressures were minimal, a contact resistance of 30 W/m^2K was used.

Temperature versus time curves for the molybdenum and adjacent Si_3N_4 nodes from this simulation are presented in Figure 5. Note that the temperature of the molybdenum is about 600 ^oC higher than the Si_3N_4; the molybdenum is just over its melting point, and the Si_3N_4 is just below its decomposition temperature. These are the conditions that we see in the experiments, and are the non-equilibrium conditions that lead to bonding.

CONCLUSIONS

These experiments demonstrated the feasibility of melting refractory metals with a high-energy electron beam, and using this layer as a braze material in buried interfaces between Si_3N_4 pieces. The following conclusions can be drawn from the experiments. The best incident beam power density for Si_3N_4-Mo-Si_3N_4 bonding, over the limited range of these tests, appears to be in the range of 1000- 2000 W/cm^2, where the severe effects of ceramic cratering and damage are minimized, and the best temperature range for reactive bonding occurs. The best incident beam power density for Si_3N_4-Pt-Si_3N_4 is around 600 W/cm^2. Reactions between the metal and ceramic produced silicides that bond the metal to the ceramic.

We observed compressive shear strengths up to 28 MPa, in the low end of the range of strengths achieved for joints fabricated using conventional techniques (30-320 MPa). These strength results are for our initial experiments and are expected to improve significantly once we are able to achieve a more uniform beam profile.

Further experiments will be conducted to provide a uniform beam over the entire sample, and optimize (reduce) the peak power levels used in this experiment. With these experiments, we hope to produce higher uniformity of bonding, higher strength, and lower damage to the ceramic material.

REFERENCES

[1] K. Suganuma, "Joining Non-Oxide Ceramics," pp. 523-531 in ASM Handbook, Vol. 4, Glasses and Ceramics, ASM International, (1991).

[2] H. A. Hokanson, S. L. Rogers, and W. I. Kern, "Electron Beam Welding of Alumina," Ceram. Ind. Mag., 81, p. 44 (1963).

[3] R. W. Rice, "Welding of Ceramics," NRL-7085 (1970).

[4] K. Mohammed Jasim, R. D. Rawlings, and D. R. F. West, "Operating regimes for laser surface engineering of ceramics," J. Mater. Sci., 27, 1937-1946 (1992).

[5] Herbert L. Anderson, Editor, "Heat Transfer," Physics Vade Mecum, American Institute of Physics, New York, pp. 42-44, (1981).

[6] J. C. Anderson, K. D. Leaver, R. D. Rawlings, and J. M. Alexander, Materials Science, Chapman and Hall, New York,, pp. 313-315, (1990).

[7] J. J. Petrovic, "$MoSi_2$-Based High Temperature Structural Silicides," MRS Bulletin, July 1993, pp. 35-40, (1993).

[8] W. Siming and W. Shenghong, "Diffusion Bonding of Silicon Nitride Engineering Ceramics to Metals Using Hot Isostatic Pressing," Hot Isostatic Pressing - Theory Appl. Proc., 339-344 (1992).

[9] E. Heikinheimo, A. Kodentsov, J. A. Van Beek, J. T. Klomp, and F. J. J.Van Loo, "Reactions in the Systems Mo-Si_3N_4 and Ni-Si_3N_4," Acta Metall. Mater. 40, Suppl. pp. S111-S119 (1992).

[10] O. M. Akselsen, "Review - Advances in Brazing of Ceramics," J. Mater. Sci., 27 [8] (1992).

[11] S. Kang, E. M. Dunn, J. H. Selverian, H. J. Kim, "Issues in Ceramic-to-Metal Joining: An Investigation of Brazing a Silicon Nitride-Based Ceramic to a Low-Expansion Superalloy," Ceram. Bull., 68 [9] 1608 (1989).

[12] H. Mizuhara and K. Mally, "Ceramic-to-Metal Joining with Active Brazing Filler Metal," Weld. J., 64 [10] 27-32 (1985).

[13] J. H. Selverian and S. Kang, "Ceramic-to-Metal Joints: Part II - Performance and Strength Prediction," Bulletin of the American Ceramic Soc., 71 [10] 1511-1520 (1992).

[14] J. A. Halbleib, R. P. Kensek, G. D. Valdez, S. M. Seltzer, and M. J. Berger, "ITS: The Integrated TIGER Series of Electron/Photon Transport Codes - Version 3.0." IEEE Trans. Nucl. Sci., Vol. 39, pp. 1025-1030, (1992).

[15] P/THERMAL User's Manual, PDA Engineering, PATRAN Division, Costa Mesa, CA, (1989).

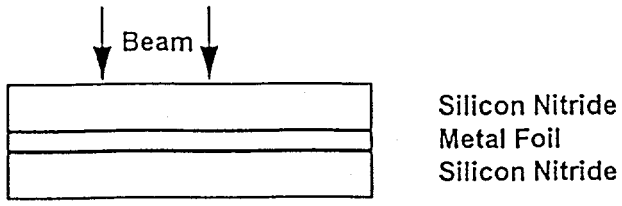

Fig. 1 Beam absorption in multi-layered materials, in this case a layer of platinum foil between two ceramic slabs.

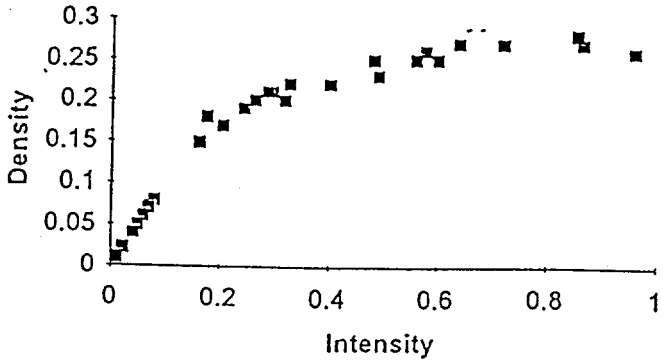

Fig. 2 Measured optical density versus beam intensity for Pyrex glass plates (0.32 cm thickness) exposed to 10 MeV electrons.

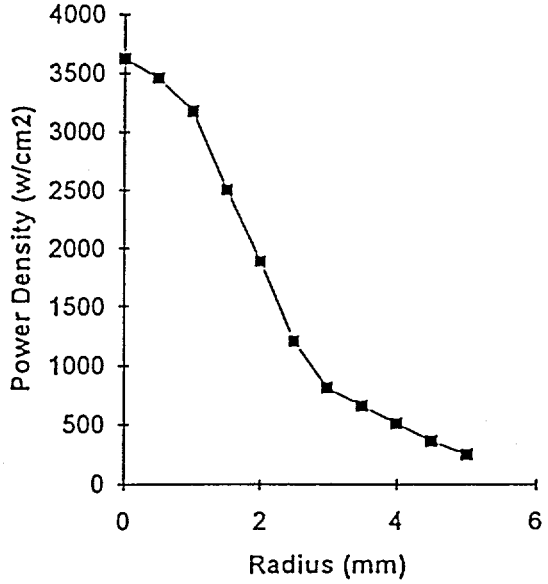

Fig. 3 Beam power density versus radius for "standard conditions": 10 MeV, 0.19 A peak current, 6 μs pulse width, 70 Hz repetition rate.

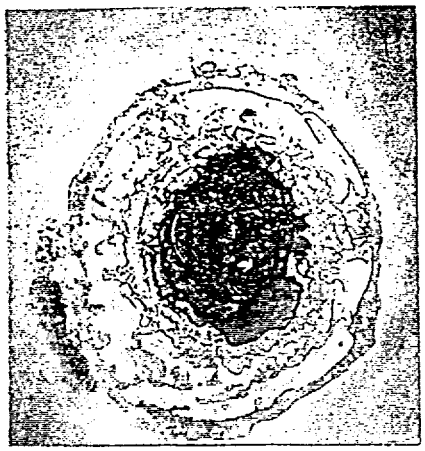

Fig. 4 a) Melting of Mo in a Si_3N_4 - Mo -Si_3N_4 sample (Test 10.3) exposed to the electron beam at 4064 W/cm^2 for 30 sec and at 5225 W/cm^2 for 5 sec. Some damage to the Si_3N_4 in the region of metal melting is evident.

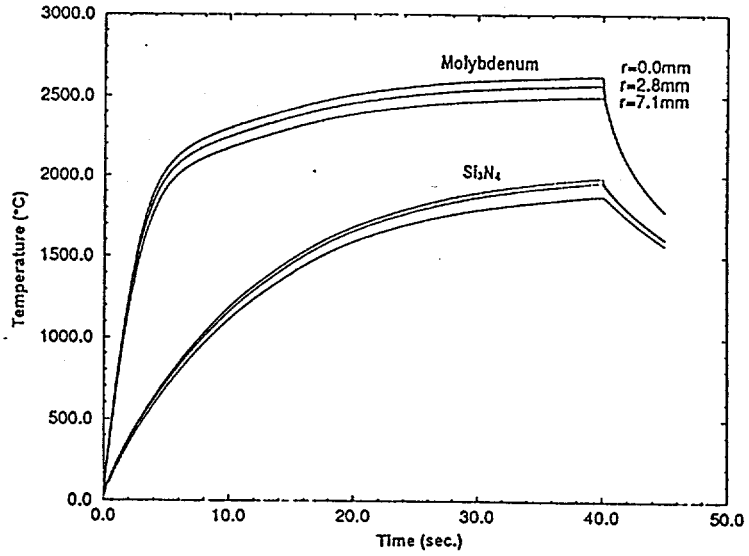

Fig. 5 Temperature versus time for the molybdenum and adjacent Si_3N_4 grid nodes, for the geometry from Fig. 1.